

## Ratcheting of Granular Materials

F. Alonso-Marroquín and H. J. Herrmann

ICAI, University of Stuttgart, Pfaffenwaldring 27, 70569 Stuttgart, Germany

(Received 30 April 2003; published 6 February 2004)

We investigate the quasistatic mechanical response of soils under cyclic loading using a discrete model of randomly generated convex polygons. This response exhibits a sequence of regimes, each one characterized by a linear accumulation of plastic deformation with the number of cycles. At the grain level, a quasiperiodic ratchetlike behavior is observed at the contacts, which excludes the existence of an elastic regime. The study of this slow dynamics allows exploration of the role of friction in the permanent deformation of unbound granular materials subjected to cyclic loading.

DOI: 10.1103/PhysRevLett.92.054301

PACS numbers: 45.70.Cc, 61.43.Bn, 83.10.Gr, 83.80.Nb

A particularly intriguing phenomenon in driven systems is the so-called ratchet effect. There is already an extensive body of work on this subject, driven by the need to understand biophysical systems such as molecular motors [1] and certain mechanical and electrical rectifiers [2]. The classic ratchet is a mechanical device consisting of a pawl that engages the sloping teeth of a wheel permitting motion in one direction only. Ratchetlike motion has been proposed as a mechanism to explain the convective motion and size segregation in vibrated granular materials [3]. The concept of *ratcheting* has been also introduced in soil mechanics, to describe the gradual accumulation of permanent deformation in granular materials subjected to cyclic loading [4]. Rutting and cracking of pavement are direct consequences of the ratcheting deformation of the roadbed [5].

Most theoretical models of unbound granular materials postulate a purely elastic regime where deformation is completely linear and reversible [6]. This assumption is contradicted by recent experiments, which show ratcheting under small loading cycles, even when there is no wearing of the individual grains [4]. A clue for the micro-mechanical origin of this effect is provided in [7]. These investigations emphasize the large fluctuations of the contact forces and their convoluted spatial structure. The strong broadening of the tangential forces gives rise to a large number of contacts that reach the sliding condition, even when the sample is isotropically compressed. Already under extremely small loading, these sliding contacts produce irreversible deformations in the sample [8]. In this Letter these issues are addressed in a well-defined system, and we find overall ratcheting behavior due to the collective sliding of the individual contacts.

We will numerically study the cyclic loading response of a two-dimensional granular model material. The interparticle forces include elasticity, viscous damping, and friction with the possibility of slip. The system is driven by applying vertical stress cycles while keeping the horizontal confining stress constant. In quasistatic regime we detect ratcheting motion at the sliding contacts even for small loading amplitudes. These ratchets produce long

time regimes with a constant rate of accumulation per cycle of permanent deformation, excluding the existence of an elastic regime.

The samples are represented by assemblies of polygons which are generated by using a simple version of Voronoi tessellation: First, we set a random point in each cell of a regular square lattice of side  $\ell$ . Then, each polygon is constructed assigning to each point that part of the plane that is nearer to it than to any other point [9]. This method gives a diversity of areas of polygons following a Gaussian distribution with mean value  $\ell^2$  and variance of  $0.36\ell^2$ . The number of edges of the polygons is distributed between 4 and 8 for 98.7% of the polygons, with a mean value of 6.

To obtain samples with volume fractions lower than one, the polygons are placed randomly inside a rectangular frame consisting of four walls. Then, a gravitational field is applied and the sample is allowed to consolidate. The external load is imposed by applying a force  $\sigma_x H$  and  $\sigma_y W$  on the horizontal and vertical walls, respectively. Here  $\sigma_x$  and  $\sigma_y$  are the vertical and horizontal stresses.  $H$  and  $W$  are the height and the width of the sample. First, the sample is isotropically compressed until the pressure  $p_0$  is reached. When the velocity of the polygons vanishes gravity is switched off. Then, the vertical stress  $\sigma_x = p_0$  is kept constant and horizontal stress is modulated as  $\sigma_y = p_0 + \Delta\sigma_y[1 - \cos(\pi t/t_0)]/2$ . This smooth modulation is chosen in order to minimize the acoustic waves produced during the load-unload transition.  $\Delta\sigma_y$  is chosen between  $0.001p_0$  and  $0.4p_0$ . These values should be compared to the maximal stress during the biaxial test, which is around  $0.75p_0$  in this model.

The interaction between the polygons is modeled as follows: when two polygons overlap, two points can be defined by the intersection of their edges. The segment connecting these two intersection points defines the contact line. The contact force is separated as  $\vec{f}^c = \vec{f}^e + \vec{f}^v$ , where  $\vec{f}^e$  and  $\vec{f}^v$  are the elastic and viscous contribution.

The elastic part of the contact force is decomposed as  $\vec{f}^e = f_n^e \hat{n}^c + f_t^e \hat{t}^c$ , where  $\hat{n}^c$  and  $\hat{t}^c$  are the unitary vectors

perpendicular and parallel to the contact line. The *normal elastic force* is calculated as  $f_n^e = -k_n A/L_c$ , where  $k_n$  is the normal stiffness,  $A$  is the overlapping area, and  $L_c$  is a characteristic length of the polygons pair [9].

The *friction force* is given by an elastic force  $f_t^e = -k_t \Delta x_t$  proportional to the elastic displacement at each contact. Here  $k_t$  is the tangential stiffness. The elastic displacement  $\Delta x_t$  is calculated as the time integral of the tangential velocity of the contact during the time where the condition  $|f_t^e| < \mu f_n^e$  is satisfied, where  $\mu$  denotes the friction coefficient. The *sliding condition* is imposed keeping this displacement constant when  $|f_t^e| = \mu f_n^e$ .

The *viscous force* is given by  $\vec{f}^v = -m\nu\vec{v}^c$ , where  $m$  is the effective mass of the polygons in contact and  $\nu$  is the coefficient of viscosity. This force reduces the acoustic waves produced during the loading. Inertia effects were excluded by using a very long time of loading. Indeed, doubling it affects the strain response by less than 5%. This corresponds to the quasistatic approximation.

The parameters of our model have been reduced to a minimum set of dimensionless parameters: The period of cyclic loading  $t_0$  is chosen 4000 times the characteristic period of oscillation  $t_s = \sqrt{k_n/\rho\ell^2}$ , where  $k_n$  is the normal stiffness of and  $\rho$  the density of the grains. The relaxation time  $t_r = 1/\nu$  is chosen 10 times  $t_s$ . The tangential stiffness is  $k_t = 0.33k_n$ ; the initial pressure  $p_0 = 0.001k_n$  and the friction coefficient  $\mu = 0.25$ . Finally,  $t_s = 2.5 \times 10^{-5}$  s and  $k_n = 160$  MPa. A fifth-order predictor-corrector algorithm is used to solve the equations of motion.

In order to calculate the strain, we select the polygons whose centers of mass are less than  $10\ell$  from the center of the sample. Then, the strain tensor is calculated as the displacement gradient tensor averaged over the area enclosed by the initial configuration of these polygons. From the eigenvalues  $\epsilon_1$  and  $\epsilon_2$  of the symmetric part of this tensor we obtain the shear strain as  $\gamma = \epsilon_1 - \epsilon_2$ . The volume fraction is calculated as  $\Phi = (V_p - V_0)/V_b$ , where  $V_p$  is the sum of the areas of the polygons,  $V_0$  the sum of the overlapping area between them, and  $V_b$  the area of the rectangular box. The initial volume fraction is  $\Phi_0 = 84.49 \pm 0.05\%$ .

Figure 1(a) shows the relation between the stress  $\sigma_y$  and the shear strain  $\gamma$  in the case of a loading amplitude  $\Delta\sigma_y = 0.424p_0$ . This relation consists of open hysteresis loops which narrow as consecutive load-unload cycles are applied. This hysteresis produces an accumulation of strain with the number of cycles which is represented by  $\gamma_N$  in Fig. 1(b). We observe that  $\gamma_N$  consists of short time regimes, with rapid accumulation of plastic strain, and long time *ratcheting* regimes, with a constant accumulation rate of plastic strain of around  $2.4 \times 10^{-6}$  per cycle.

The relation between the stress and the volume fraction is shown in Fig. 1(c). This consists of asymmetric compaction-dilation cycles leading to compact during the cyclic loading. This compaction is shown in Fig. 1(d).

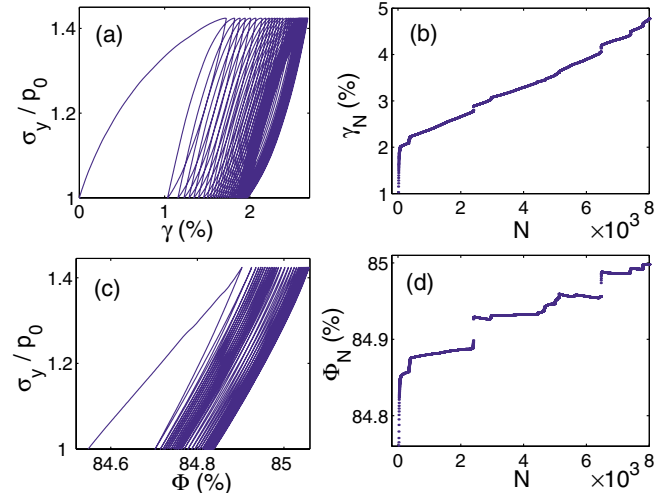


FIG. 1 (color online). (a) Horizontal stress versus shear strain in the first 40 cycles; (b) permanent (plastic) strain  $\gamma_N$  after  $N$  cycles versus the number of cycles; (c) stress against the volume fraction in the first 40 cycles; (d) volume fraction  $\Phi_N$  after  $N$  cycles versus number of cycles.

We observe a slow variation of the volume fraction during the *ratcheting* regime, and a rapid compaction during the transition between two ratcheting regimes, whereas the slope of  $\gamma_N$  shows no dependency on the compaction level of the sample. The evolution of the volume ratio seems to be rather sensitive to the initial random structure of the polygons. Even so we found that after  $8 \times 10^3$  cycles the volume fraction still slowly increases in all the samples, without reaching the saturation level.

This extremely slow dynamics in the evolution of the granular packing shows an astonishing analogy with the behavior of glassy systems [10,11]. Even more surprising is that no elastic regime is detected by decreasing the

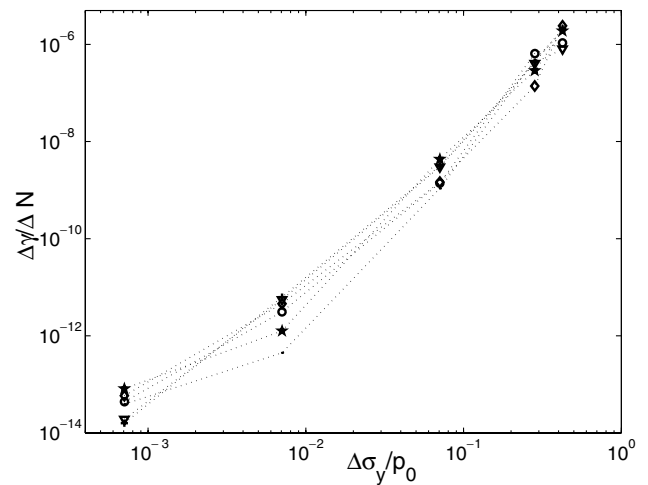


FIG. 2. Plastic deformation per cycle for different loading amplitudes. The calculations are performed on six different samples, each with 400 polygons.

amplitude of the loading cycles. Figure 2 shows the accumulation rate of strain  $\Delta\gamma/\Delta N$  for different loading amplitudes  $\Delta\sigma_y$ . A constant accumulation of strain is observed during the cyclic loading, even when the amplitude is as slow as  $10^{-3}$  times the applied pressure.

Because of the particular strong fluctuations in the granular materials, the existence of these ratcheting regimes appears to be somewhat counterintuitive. However, we will show that this effect arises from the large fluctuations of the contact forces and the quasiperiodic evolution of the forces at the sliding contacts. Figure 3(a) shows the distribution of contact forces in a sample which has been isotropically compressed. The components of the force are limited by the condition  $|f_t| \leq \mu f_n$ , where  $\mu$  is the friction coefficient. Most of the contacts satisfy the elastic condition  $|f_t| < \mu f_n$ , but due to the heterogeneities, some contacts are able to reach the sliding condition  $|f_t| = \mu f_n$  during the compression. Under extremely small stress cycles these contacts slide, causing irreversible motion between the grains. Those sliding contacts carry most of the permanent deformation of the granular assembly during the cyclic loading. Opening and closure of contacts are quite rare events, and the coordination number of the packing keeps approximately its initial value  $4.43 \pm 0.08$  throughout the simulation.

After some loading cycles the contact forces become almost periodic in time, even at the sliding contacts. Two different sliding modes are shown in Fig. 3: (b) a contact sliding forward in the load phase and backward in the unload one and (c) a contact sliding in the load phase and sticking in the unload one. A measure of the plastic deformation of the sliding contact is given by  $\xi = (\Delta x_t^c - \Delta x_t^e)/\ell$ , where  $\Delta x_t^c$  and  $\Delta x_t^e$  are the total and the

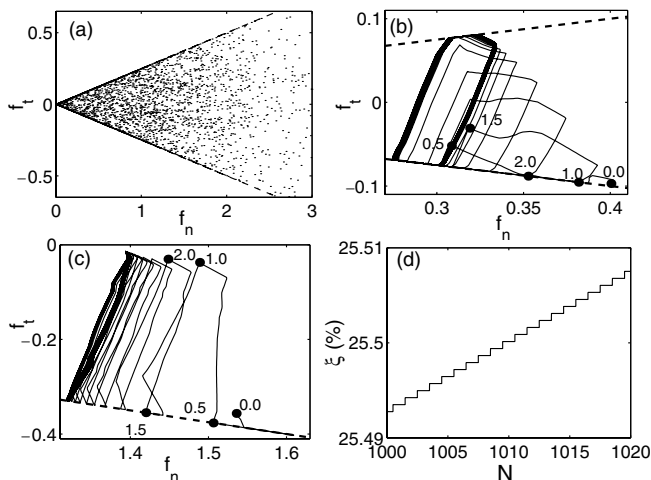


FIG. 3. (a) Each point represents the normal and tangential force at one contact normalized by  $\ell p_0$ . The dashed line shows the sliding condition  $|f_t| = \mu f_n$ ; (b) and (c) show trajectories of the contact force of two selected sliding contacts. The dots denote the times  $t = 0, 0.5t_0, \dots, 2t_0$  in unit of the period  $t_0$ ; (d) shows plastic deformation  $\xi$  at the contact shown in (c).

elastic part of tangential displacement at the contact. Figure 3(d) shows the plastic deformation  $\xi$  of the sliding contact shown in (c). Because of the load-unload asymmetry of the contact force loop, a net accumulation of plastic deformation is observed in each cycle. This is given by a slip-stick mechanism which resembles mechanical ratchets.

It is interesting to see the spatial correlation of these ratchets. Figure 4 shows a snapshot of the field of plastic displacement per cycle at the contacts inside of the specimen. We see that correlated displacements coexist with a strongly inhomogeneous distribution of amplitudes. Localized slip zones appear periodically in time during each ratcheting regime. This behavior is reflected in a constant displacement per cycle of each grain during the ratcheting regime. Big displacements are observed in the transition between two ratcheting regimes, which yield the destruction of some slip zones and the creation of new ones. Moreover, we notice that these ratchets are found as well at the boundaries as in bulk material, without the layering effects observed in vibrated granular materials [3].

Starting from a micromechanical investigation one may directly model the hysteresis loops of this ratcheting behavior. A first step is to establish the correlation between the dynamics of the sliding contacts and the evolution of the stiffness of the material. The latter one is given by the slope of the stress-strain curve in Fig. 1(a). The time evolution of the fraction  $n_s = N_s/N_c$  of sliding

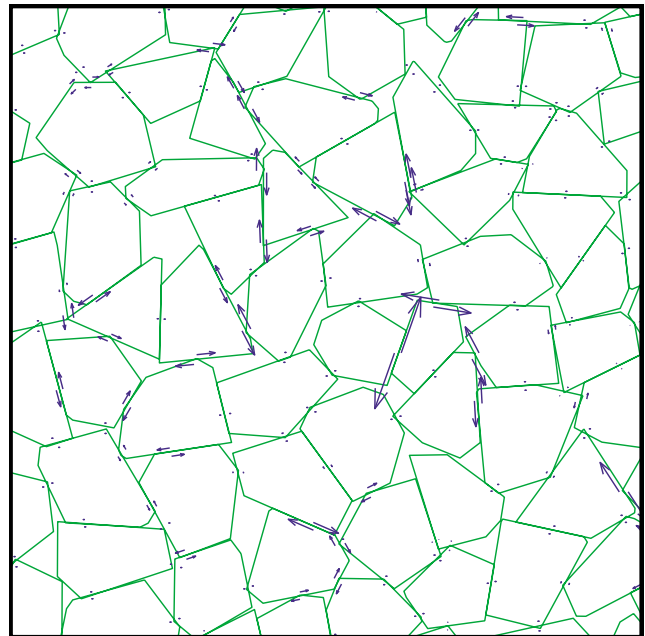


FIG. 4 (color online). The arrows represent the field  $\vec{u}$  of the plastic deformations accumulated at the contacts during one cycle:  $u = 500(\xi_{N+1} - \xi_N)$ , where  $\xi_N$  is the plastic displacement after  $N$  cycles.

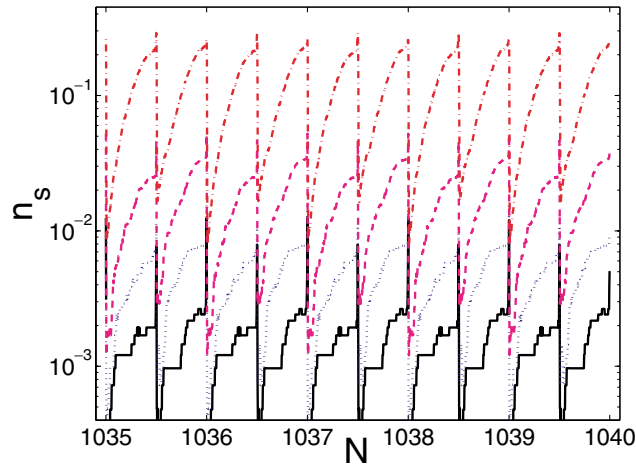


FIG. 5 (color online). Fraction of sliding contacts  $n_s$  in the ratcheting regime for  $\Delta\sigma_v/p_0 = 0.424$  (dash-dotted line), 0.0707 (dashed line), 0.00707 (dotted line), and 0.000707 (solid line)

contacts is shown in Fig. 5. Here  $N_s$  is the number of sliding contacts and  $N_c$  is the total number of contacts. During each loading phase, the number of sliding contacts increases, giving rise to a continuous decrease of the stiffness as shown in Fig. 1(a). An abrupt reduction in the number of sliding contacts is observed at the transition from load to unload, producing a discontinuity in the stiffness. We can see also that some contacts reach almost periodically the sliding state even for extremely small loading cycles. The ratchetlike behavior of these contacts produces a net displacement per cycle of the hysteretic stress-strain loop leads to a ratcheting response for small cycles.

The fact that there is no evidence of an elastic regime suggests that the hysteresis of the granular materials cannot be described by the Drucker-Prager theory [6]. Actually, the deficiencies of this theory have been addressed in the experimental investigation of soil deformation [12]. Ten years ago, the *hypoplastic model* was formulated in order to mend these deficiencies. This continuum theory has been supported by the experimental evidence that any load involves plastic deformation [13].

The hypoplastic approach of granular materials requires introducing new ingredients into the current micromechanical description. The traditional fabric tensor, measuring the distribution of the orientation of the contacts, cannot fulfill this role, because it does not make a distinction between elastic and sliding contacts [14]. New structure tensors taking into account the statistics of the sliding contacts, must be introduced to give a micromechanical basis to the granular ratcheting. The identification of these internal variables and the determination of their evolution equations and their connection

with the macroscopic variables would be a key step in the development of an appropriate continuous description of granular soils.

To conclude, we have performed a grain scale investigation of the cyclic loading response of a polygonal packing. We have shown the existence of long time regimes with a constant accumulation of plastic deformation per cycle, due to ratcheting motion at the sliding contacts. This phenomenon may have deep implications in the study of the permanent deformation of soils subjected to cyclic loading. More precisely, it may be necessary to introduce internal variables in the constitutive relations, connecting the dynamics of the sliding contacts with the evolution of the continuous variables during cyclic loading.

At this time, a comparison of the dynamic simulations with realistic situations is limited by the computer time of the simulations. Using a computer with a 2.4 GHz processor we are able to simulate only 20 cycles per hour. However, further investigations of the role of the stiffness, the initial stresses, and the inertial effects on this ratcheting behavior are currently feasible.

We thank G. Gudehus, P. Cundall, D. Potyondy, A. Schuenemann, J. Gallas and S. McNamara for helpful discussions and acknowledge the support of the DFG Project *Modellierung kohäsiver Reibungsmaterialien* and the European DIGA Project No. HPRN-CT-2002-00220.

- 
- [1] J. Howard, *Nature (London)* **389**, 561 (1997).
  - [2] P. Reimann, *Phys. Rep.* **361**, 57 (2002).
  - [3] H. M. Jaeger, and S. R. Nagel, *Rev. Mod. Phys.* **68**, 1259 (1996).
  - [4] G. Festag, dissertation, TU Darmstadt (unpublished).
  - [5] F. Lekarp, A. Dawson, and U. Isacsson, *J. Transp. Eng.* **126**, 76 (2000).
  - [6] D. C. Drucker, and W. Prager, *Q. Appl. Math.* **10**, 157 (1952).
  - [7] F. Radjai, M. Jean, J. J. Moreau, and S. Roux, *Phys. Rev. Lett.* **77**, 274 (1996).
  - [8] F. Alonso-Marroquin, and H. J. Herrmann, *Phys. Rev. E* **66**, 021301 (2002).
  - [9] F. Kun, and H. J. Herrmann, *Phys. Rev. E* **59**, 2623 (1999).
  - [10] A. J. Liu and S. Nagel, *Nature (London)* **396**, 21 (1998).
  - [11] M. Nicolas, P. Duru, and O. Pouliquen, *Eur. Phys. J. E* **3**, 309 (2000).
  - [12] *Constitutive Relations of Soils*, edited by G. Gudehus, F. Darve, and I. Vardoulakis (Balkema, Rotterdam, 1984).
  - [13] D. Kolymbas, *Arch. Appl. Mech.* **61**, 143 (1991).
  - [14] R. J. Bathurst and L. Rothenburg, *J. Appl. Mech.* **55**, 17 (1988).